

WITHDRAWN: A global carbon and nitrogen isotope perspective on modern and ancient human diet

Michael I Bird

michael.bird@jcu.edu.au

James Cook University <https://orcid.org/0000-0003-1801-8703>

Stefani Crabtree

Utah State University <https://orcid.org/0000-0001-8585-8943>

Jordahna Haig

James Cook University <https://orcid.org/0000-0003-1350-522X>

Sean Ulm

James Cook University <https://orcid.org/0000-0001-6653-9963>

Christopher Wurster

James Cook University

Article

Keywords: diet, isoscapes, stable isotope, palaeodiet, isotope forensics

Posted Date: August 25th, 2020

DOI: <https://doi.org/10.21203/rs.3.rs-61331/v1>

License:   This work is licensed under a Creative Commons Attribution 4.0 International License.

[Read Full License](#)

Additional Declarations: There is **NO** Competing Interest.

Version of Record: A version of this preprint was published at Proceedings of the National Academy of Sciences on May 3rd, 2021. See the published version at <https://doi.org/10.1073/pnas.2024642118>.

EDITORIAL NOTE:

The full text of this preprint has been withdrawn by the authors while they make corrections to the work. Therefore, the authors do not wish this work to be cited as a reference. Questions should be directed to the corresponding author.

Abstract

Stable carbon and nitrogen isotope analyses are widely used to infer diet and mobility in ancient and modern human populations, potentially providing a means to situate humans in global food webs. We collated 13,533 globally distributed analyses of ancient and modern human collagen and keratin samples. We converted all data to a common 'Modern Diet Equivalent' reference frame to enable direct comparison between ancient and modern human diets and the natural environment. This approach reveals a broad diet in ancient times, consistent with the human ability to consume opportunistically as extreme omnivores within complex natural food webs and across multiple trophic levels in every terrestrial and many marine ecosystems on the planet. In stark contrast, dietary breadth across modern non-subsistence populations has dramatically compressed by two-thirds, largely as a result of the rise of industrial agriculture and animal husbandry practices, as well as the globalization of food distribution networks.

Introduction

Homo sapiens are the most widely distributed terrestrial mammal on the planet. Over the course of the Holocene, modern human range has extended to all continents, to the farthest islands of every ocean, and above the polar circles. The ability to rapidly adapt to newly encountered environments via technological and cultural innovation, that manifested ultimately in changes to our own genome, enabled this breathtaking range of expansion¹. Our capacity for successful innovation is tightly coupled to our ability to consume as 'extreme omnivores', that is, across multiple trophic levels (from the base of a food web to filling the niche of apex predator²⁻⁴). The development of agriculture, animal husbandry, urbanized societies and commercial trade progressively allowed us to engage in niche construction of increasing complexity and extent^{5,6}. As we permanently extended our range to above the Antarctic Circle in the 20th century, we progressively extended our capacity for advanced ecosystem engineering, thereby achieving a high degree of control over the production and distribution of our food supply across the globe^{6,7}.

The archaeological record documents, in a temporal framework, our expansion into new habitats, newly developed technologies, changing cultural practices, and the food that sustained us⁸. While the physical remains of our diets, such as bones and charred plant remains, provide direct evidence of diet, not all foodstuffs are so well-preserved. Moreover, such direct evidence does not indicate the proportion of different components that were consumed. A challenge in recreating past dietary components lies in accounting for taphonomic processes that may impact different organisms at different rates, leading to underrepresentation of some important taxa². In contrast, the stable carbon and nitrogen isotope composition of human tissue (mostly collagen and keratin) has been investigated over the last several decades as a proxy for the proportions of different potential dietary components enabling an accounting for taphonomy⁹. Carbon isotope composition ($\delta^{13}\text{C}$ value) provides an indication of relative contributions of aquatic and/or terrestrial sources of carbon in the diet. Nitrogen isotope composition ($\delta^{15}\text{N}$ value) is

used to draw inferences regarding both the protein source and trophic level of an individual in the months or years before their death¹⁰.

To date, studies involving regional patterns in the stable isotope composition of ancient human remains (mostly bone collagen that can be well-preserved) have tended to focus on regional-scale variations during the Holocene, with the intent of determining wholesale changes in subsistence strategies (e.g. agriculture and pastoralism), changing technological innovation, and social practices and structures^{11–13}. Although interpretation can sometimes be straightforward when observed differences are large, smaller differences are complicated by the complexities associated with disentangling the ecosystem processes driving C and N isotope fractionation within the food webs supporting human diet^{13,14}.

A parallel body of stable isotope research has been conducted on the stable isotope composition of the tissues of contemporary humans^{15–18}. This research has mostly focused on non-invasive nail and hair keratin, to examine the physiological processes in the human body, to deduce the recent movements of individuals¹⁹, or to identify locations for repatriation of human remains²⁰. Substantial effort has been directed towards developing a spatial understanding of the controls on the stable isotope composition of modern human tissues, mostly as a consequence of the potential forensic application of this type of research^{18,21}.

Archaeological and modern stable isotope results on human tissues are readily comparable for multiple reasons (see Methods), yet there has been no attempt to interrogate the full record of dietary breadth and change for a globally distributed, omnivorous species, from the Holocene to recent times. To address this, we collated isotope compositions of collagen, hair and nail keratin from three worldwide populations: modern urban (dates AD 1910-2020; see Methods), modern subsistence (dates AD 1910-2020), and ancient (before AD 1910). For the first time we calibrate all isotope compositions to their modern diet equivalent in order to directly compare modern and ancient distributions on a common scale. We show that the industrialized food system is vastly compressed in niche-space and vastly less resilient compared with modern subsistence and ancient diets that are underpinned by complex food-webs.

Results

We systematically collated (N = 6,879) globally distributed analyses of 'ancient' (pre-1910; see Methods) archaeological bone collagen. We further collated analyses from studies of modern (post-1910) hair and nail keratin from populations of subsistence foragers, fishers, agriculturalists and pastoralists (N = 1,044), and urban populations (N = 5,610). In order to compare populations, we adjusted all measured values onto a common frame of reference, that being the equivalent $\delta^{13}\text{C}$ and $\delta^{15}\text{N}$ values of hair keratin in 2010 or Modern Keratin Equivalent (MKE). We then used the accepted fractionations between human hair keratin and diet to calculate the Modern Diet Equivalent ($\delta^{13}\text{C}_{\text{MDE}}$ value) and ($\delta^{15}\text{N}_{\text{MDE}}$) values for all samples in 2010 (see Methods for detail).

This approach has the advantage of allowing direct comparison of all results against the framework of our much more detailed contemporary understanding of stable isotope systematics in the modern biosphere. Exploiting this link between ancient and modern requires the assumption that the environmental conditions that drive the food webs that humans rely upon, wherever they are, have remained stable and that the past can be mapped onto the present. While there have been changes in climate and environment during the Holocene these have been relatively muted, with most larger-scale landscape change resulting from human intervention in recent times, and not changes in underlying environmental drivers²².

Figure 1 presents all modern and ancient data on the common dietary scale relative to 2010. The total range across all ancient samples for $\delta^{13}\text{C}_{\text{MDE}}$ value is -31.4 to -10.4 ‰ and for $\delta^{15}\text{N}_{\text{MDE}}$ value is -2.3 to +22.3 ‰. Isotope values are not randomly distributed across the range of potential paired values instead concentrated in a rough trapezoid representing the full range of dietary possibilities available in ancient times. The stable isotope compositions of modern individuals living on a ‘traditional’ subsistence diet are remarkably similar, with $\delta^{13}\text{C}_{\text{MDE}}$ values that range from -30.1 to -11.7 ‰ and $\delta^{15}\text{N}_{\text{MDE}}$ values from -0.4 to +15.1 ‰. These values cover most— but not all— of the range covered by the ancient population. This is not surprising, as the number of studies are far fewer ($n = 10$), and large regions of the globe are no longer occupied by any individuals living by traditional subsistence means. By contrast, the modern urban population is highly compressed with means for analyses grouped by countries for modern individuals living on a globalized diet ranging from -24.2 ‰ (for the subset of vegans in the United Kingdom²³ to -18.7 ‰ (for the population sampled in Iran and Pakistan¹⁸ for $\delta^{13}\text{C}_{\text{MDE}}$ values. $\delta^{15}\text{N}_{\text{MDE}}$ mean values range from +0.45 ‰ (for the subset of vegans in Gothenberg, Germany²⁴ to +5.7 ‰ (Port Moresby, Papua New Guinea²⁵. The Papua New Guinea urban population is unique in the modern dataset for the maintenance of a close connection to subsistence foodstuffs compared the other populations in the dataset.

Discussion

The outer trapezoid-shaped bounds in the relationship between $\delta^{13}\text{C}_{\text{MDE}}$ value and $\delta^{15}\text{N}_{\text{MDE}}$ value in Figure 1 are constrained fundamentally by the range of isotope compositions possible at the base of food webs globally²⁶. In the terrestrial biosphere, this range is driven primarily by the established relationships between climate and the $\delta^{13}\text{C}_{\text{MDE}}$ value and $\delta^{15}\text{N}_{\text{MDE}}$ value of primary production^{27–31}. The climate-driven relationship is modulated regionally and locally by edaphic factors such as soil type³² and in some cases by environment-specific phenomena such as the incorporation of low $\delta^{13}\text{C}_{\text{MDE}}$ value carbon from methane oxidation into some lacustrine and wetland food webs³³. In the ocean, $\delta^{13}\text{C}_{\text{MDE}}$ and $\delta^{15}\text{N}_{\text{MDE}}$ values at the base of the food web also vary in broadly predictable ways, controlled primarily by global ocean circulation and productivity^{34,35}, modulated at the local scale by interactions with the terrestrial biosphere, for example, through the incorporation of seabird guano into the base of local food webs³⁶.

Additional to these fundamental controls on the stable isotope composition of primary production are local modifications possible through processes specific to particular environmental niches. These include trophic enrichment in both $\delta^{13}\text{C}_{\text{MDE}}$ and $\delta^{15}\text{N}_{\text{MDE}}$ values through complex food web interactions^{26,37,38} ultimately by the choice between, and manipulation of, the dietary possibilities available to humans, in the context of societal and technological constraints, at a particular time and place^{10,39-41}. All of the space within the outer bounds delineated by the range observed in primary production is occupied to a greater or lesser degree by isotope results from ancient humans, from single individuals to large populations of individuals, indicative of our impressive capacity for adaptive omnivory at the global scale. The observation that the results for modern individuals on a subsistence diet occupies much the same isotope-space as the results for the (much larger) ancient sample group indicates that the conversion of all the results to a 'modern' diet in 2010 has successfully enabled the comparison between ancient and modern human diet (Figure 1).

The most striking difference across the entire dataset is the compressed range of modern non-subsistence diets compared to modern subsistence and ancient isotope values. The $\delta^{15}\text{N}_{\text{MDE}}$ values of modern subsistence diets imply consumption across trophic levels from around 1 (plant only) to ~4-5 in populations reliant dominantly on high latitude marine resources (e.g. Greenland), assuming an average trophic enrichment factor of 4‰ (see Methods). Some ancient populations appear to be consuming at even higher trophic levels, though the highest $\delta^{15}\text{N}_{\text{MDE}}$ values $>+15\text{‰}$ relate to sea bird guano fertilization of crops in arid South America⁴².

In contrast, the modern human range of trophic levels, determined by nitrogen isotope composition (see Methods) is much narrower, from $<\sim 1.5$ (for vegans and vegetarians) to an average of $\sim 1.75-2.5$ for most generally omnivorous populations, aggregated by country (see Methods for calculation). This range is consistent with the global average isotopic human trophic level, as indicated by direct measures of diet, aggregated by country, of 2.21, similar to the trophic level in a natural food web of anchovies and pigs⁷. In part, the observed compression in the range of modern non-subsistence populations is the result of improvement in diet in developing countries, such that trophic levels in developing countries have increased, thereby converging somewhat with those of developed countries over time⁷. In part, the observed compression is the result of a general decrease in the trophic level of animal and fish resources extracted for consumption from natural food webs as a result of over-exploitation in recent decades⁴³. However, the largest contribution to the apparent decrease in trophic level over the range observed in ancient populations, is likely due to the disconnection of the majority of the modern human population from complex natural food webs and their replacement by the simpler food webs⁴⁴ and flatter food chains associated with industrial agriculture and farming⁴⁵. This has effectively removed these other sources of trophic diversification from the human diet.

In the particular context of the natural nitrogen isotope cycle, modern industrial fertilizer produced from atmospheric nitrogen has a mean $\delta^{15}\text{N}$ value of $-0.2 \pm 2\text{‰}$, whereas natural soils and fertilizers, depending on environment and source have mean $\delta^{15}\text{N}$ values that range up to $+7.1\text{‰}$ ⁴⁶. Industrial

fertilizer use has increased rapidly since the 1960s and global demand now exceeds 100 Tg per year⁴⁷. This fertilizer is used in annual to sub-annual cycles of application and harvest, often in conjunction with irrigation in semi-arid regions once limited to rainfed crop production. Industrial farming has therefore effectively 'short-circuited' the suite of longer-term natural soil isotope fractionation processes leading to the higher soil $\delta^{15}\text{N}$ values that are ultimately reflected in human diets based on natural food webs. Thus, for example, modern human $\delta^{15}\text{N}_{\text{MDE}}$ values from developed countries cover a similar range to the $\delta^{15}\text{N}_{\text{MDE}}$ values of enslaved Africans in the Caribbean in the 17th to 19th centuries, whose diets were dominantly plant-based⁴⁸.

The equally dramatic compression in the range of modern $\delta^{13}\text{C}_{\text{MDE}}$ values in Figure 1 is a direct consequence of globalization. Thus, C_4 staples (e.g. sugar and maize-derived products) and C_3 staples (e.g. wheat and rice) are now cultivated well outside of their natural range using irrigation, and shipped across the world. The supermarkets that draw on these global supply chains now have a >50% share of food retailing in countries with a >US\$10,000 per capita annual income⁴⁹. While some regional differentiation between tropical and temperate countries remains in $\delta^{13}\text{C}_{\text{MDE}}$ values (Fig. 1), the modern range in values has reduced to around one-third of that observed across the ancient world.

Given the primacy of climate as the major driver of the broadest global trends in the stable isotope composition of primary production we identify three general ancient 'environments' at the global scale (Figure 1). The primary distinction is the separation of regions with an aridity index of >0.5 (sub-humid to humid) from <0.5 (arid to hyper-arid⁵⁰). 'Arid C_3/C_4 ' environments span a wide range of temperatures and here include regions with a Mediterranean climate that experience significant seasonal water stress. Humid environments are separated into the warmer regions that potentially contain C_4 biomass (Humid C_3/C_4) and colder regions that contain only C_3 biomass (Cold C_3), based on the modern distribution of C_4 biomass²⁸. Across all three categories some ancient populations also had a variable degree of access to marine and/or freshwater aquatic resources with a stable isotope composition often distinct from local terrestrial resources^{10,14,37}.

The vast majority of ancient results from regions where C_4 vegetation does not naturally occur plot along a broad diagonal from terrestrial $\delta^{13}\text{C}_{\text{MDE}}$ values of -25 to -28‰ and $\delta^{15}\text{N}_{\text{MDE}}$ values below +10‰ (e.g., Western Europe) towards a progressively more marine-influenced diet indicated by $\delta^{13}\text{C}_{\text{MDE}}$ values of >-20‰ and $\delta^{15}\text{N}_{\text{MDE}}$ values >+10‰ (e.g. Greenland and Alaska). At $\delta^{15}\text{N}$ values <10‰, $\delta^{13}\text{C}_{\text{MDE}}$ values up to ~-23‰ can still indicate a purely C_3 diet influenced by combinations of trophic enrichment as a result of meat consumption and the adoption of agricultural innovations such as manuring^{51,52} along with natural variations in discrimination by C_3 plants, particularly between trees (forest) and C_3 grasses (pasture) and associated with climate, soil type^{32,53} and land use⁵⁴. The scatter of points to higher $\delta^{13}\text{C}_{\text{MDE}}$ values >~-23‰ with relatively low $\delta^{15}\text{N}_{\text{MDE}}$ values reflect a variable degree of consumption of

introduced C₄ crops such as millet in prehistory, particularly in Eastern Europe and the Caucasus as well as individuals migrating from locations with a C₄ component in the diet in the last few centuries.

The ancient results for the Humid C₃/C₄ grouping scatter over a relatively narrower range of $\delta^{15}\text{N}_{\text{MDE}}$ values between 0 and +10‰, but span a wide range from purely C₃ (southern Japan and eastern US), to almost exclusively C₄ (Southern China and Mexico). The reliance on millet (a C₄ crop) in China is evident in the concentration of analyses with $\delta^{13}\text{C}_{\text{MDE}}$ values above -15‰, and $\delta^{15}\text{N}_{\text{MDE}}$ values below +5‰. The data for the humid C₃/C₄ grouping as a whole implies that diet across this global range is within a maximum of 3.5 isotope-calculated trophic levels. This is consistent with modern subsistence diets from populations in the environments represented in this category from the Amazon (mixed plant and fish-based diets) to Africa (mixed plant and meat). The grouping also includes island populations in the Pacific Ocean indicating that it is not possible to differentiate a marine from a purely terrestrial diet in the absence of other evidence.

The arid C₃/C₄ grouping covers the entire $\delta^{13}\text{C}_{\text{MDE}}$ isotope dietary space from exclusively C₃ plant-based (e.g. montane central USA) to largely C₄-based (e.g. central Chile). In some populations in coastal Peru $\delta^{15}\text{N}_{\text{MDE}}$ values exceed +15‰ but these very high values have been attributed to the addition of seabird guano fertilizer to crops⁴². For coastal populations, the utilization of marine resources may explain the extension to higher $\delta^{15}\text{N}_{\text{MDE}}$ values compared to the humid C₃/C₄ grouping. For populations in more arid environments it is likely that the increase in plant $\delta^{15}\text{N}_{\text{MDE}}$ values generally observed in arid environments is a contributing factor to the comparatively high $\delta^{15}\text{N}_{\text{MDE}}$ values observed in many samples in this group. In addition, it may be that in particularly hyper-arid environments such as montane central Peru, where plant biomass is not an abundant resource, populations rely to a greater extent on higher-trophic-level animal resources for their diet. As with the humid C₃/C₄ grouping it is not possible to uniquely identify an aquatic component to diet across much of the arid C₃/C₄ range in the absence of other information.

The approach adopted here, and represented conceptually in Figure 2 moves from a local archaeological framing, where interest is primarily in the proportion of potential food items in the diet of ancient individuals in that area, to a global context where humans can be placed in an ecological framework as part of, but increasingly able to manipulate, complex natural food webs. A growing body of anthropological research also examines the human place in food webs worldwide. Humans have been shown, through their hyper-omnivory and prey switching ability, consumed a wider variety of organisms than any other taxon in their respective systems^{4,55}. Modelled food webs that include humans indicate the aggregate trophic position of humans ranges from up to ~5 for offshore food webs in the Aleutian Islands⁴ to ~2.3 for modern Indigenous populations in the deserts of Western Australia⁵⁵. These trophic positions were both determined using the Short-Weighted Trophic level calculation, which allows an estimate of feeding strength from binary interactions within modelled food webs⁵⁶. The compilation of full ecologically realistic model trophic webs is laborious and therefore there are few available. However,

the broad comparability of the Short-Weighted trophic level inferences drawn from the modelling approach, with the isotope approach presented here, is encouraging.

Thus, it becomes possible to conceive of the stable isotope composition of archaeological remains as an integrated signal of human utilization and manipulation of their local food web^{55,58}. Re-casting the archaeological results into their modern diet equivalent composition then allows comparison with the much larger and more detailed datasets available for plants and fauna in modern ecosystems (Figure 2). Direct comparisons of spatially (or temporally) distinct archaeological isotope datasets can be relatively easily achieved for data collected from humid C₃ dominated terrestrial environments (as in Figure 1 above) because there is limited scope for natural variation in the isotope baselines in these environments. The extension of this approach to other, and particularly arid, environments will require a finer-grained, spatially explicit (isoscape) understanding of regional variability in isotope baselines in relation to climate and soil variables than is presently available⁵⁹.

Human populations in prehistory bolstered their resilience by being able to prey switch within complex natural food webs⁵⁸. Comparison of the ancient and modern isotope results presented here suggest that modern human food webs have become dramatically compressed as a result of the ongoing expansion of industrial agriculture and pastoralism at the expense of natural ecosystems. In turn, this is resulting in a cascade of 'rewiring' to remaining natural terrestrial and marine food webs globally⁶⁰ that can reduce complexity, and therefore the resilience, of global ecosystems in the face of accelerating environmental change^{43-45,61}.

Methods

We collated published individual stable isotope analyses of ancient human bone collagen from 127 studies with global coverage (Supplementary Table 1). Studies were identified from a systematic search of Google Scholar using combinations of the search terms *isotope, collagen, keratin, diet, ancient and archaeology*. Not all literature thus identified was available to us, and studies where primary data was not presented in the paper or supplementary information were also excluded. From the total database, we removed analyses of infant bone material, where identified, due to apparent trophic enrichment associated with breastfeeding⁶² and also removed analyses outside the recommended range of C:N ratios for collagen⁹, where reported (2.9-3.6). We did not further interrogate the techniques or instrumentation used to perform the analyses. We further collated modern analyses of hair and nail keratin from nine studies of populations still living a mostly traditional, subsistence lifestyle, and drew on an existing global synthesis of hair stable isotope composition from non-subsistence populations, aggregated by country¹⁸, augmented with data from more recent studies. As the modern non-subsistence dataset is not available as individual analyses, we report these as country means with 95 % confidence interval. We take the boundary between 'ancient' and 'modern' to be 1910, the date at which large scale production of nitrogen fertilizer by the Haber-Bosch process became possible, underpinning the rise of industrial agriculture in the 20th century.

The $\delta^{13}\text{C}$ and $\delta^{15}\text{N}$ values of all human tissues, including collagen and keratin, are modified to varying degrees from that of the diet by a number of physiological processes¹⁵⁻¹⁸, such that bone collagen, hair and nail keratin produced by an individual from the same diet do not have the same stable isotope composition. We therefore adjusted all analyses to their equivalent hair keratin isotope value using published fractionation factors. The fractionation factors applied are provided in Supplementary Table 1, and while these are uncertain, generally by $<0.5\text{‰}$, they are simple additions/subtractions uniformly applied across all data that can be amended if more precise data become available.

The $\delta^{13}\text{C}$ value of all human tissues are ultimately also dependent on the $\delta^{13}\text{C}$ value of atmospheric CO_2 at the time it was assimilated by photosynthesis. While the $\delta^{13}\text{C}$ value of the atmosphere was relatively constant through most of the Holocene ($-6.4 \pm 0.05\text{‰}$ ⁶) it decreased throughout the 20th century due to fossil fuel combustion (to -8.3‰ in 2010⁶³). As the majority of the modern samples analysed were collected in the last two decades, we take 2010 as the central reference year and adjust the $\delta^{13}\text{C}$ value of all ancient samples to their equivalent value in that year. Uncertainty around when some modern samples were actually collected results in an additional uncertainty of $\pm \sim 0.3\text{‰}$ in cases where samples were collected either very recently or in the last decade of the 20th century. The approach adopted above places all data into a directly comparable modern reference frame. We then used accepted fractionation factors between hair keratin and diet (Supplementary Table 1) to present all data as Modern Diet Equivalent isotope values ($\delta^{13}\text{C}_{\text{MDE}}$ and $\delta^{15}\text{N}_{\text{MDE}}$ values).

The final ancient dataset consists of 6879 entries. Of these, we have classified 2973 as 'Arid C_3/C_4 ', 2655 as 'Cold C_3 only' and 1251 as 'Humid C_3/C_4 '. Given the large size of the dataset, bag plots or modified bivariate boxplots (shown in Figure 1) were constructed to visualise the data distribution by way of its half-space depth or Tukey depth⁶⁴. In this, the 'bag' encloses 50% of the data points (black contour) while the modified 'loop' (coloured contours) encloses 95% of the points, allowing for the quick identification of the location and spread of the data cloud.

Trophic Level is usually defined by nitrogen isotope composition and is calculated using the following equation:

$$\text{TE} = [(\delta^{15}\text{N}_{\text{consumer}} - \delta^{15}\text{N}_{\text{producer}}) / (\text{TEF})] + 1. \quad \text{--- equation 1}$$

Where TE is trophic enrichment and TEF is trophic enrichment factor, $\delta^{15}\text{N}_{\text{consumer}}$ and $\delta^{15}\text{N}_{\text{producer}}$ are the stable values of the consumer organism, and the organism being consumed, respectively. Published Trophic Enrichment Factors range between approximately +3 and +5‰, and here we assume a value of +4‰^{10,65}.

Declarations

Reporting Summary Further information on research design is available in the Nature Research Reporting Summary linked to this article.

Code Availability There is no code associated with this research.

Data Availability All data is provided in Supplementary Table 1.

Acknowledgements

This research was undertaken by the Australian Research Council Centre of Excellence for Australian Biodiversity and Heritage (CE170100015).

Author contributions

M.I.B and C.R.W conceived the research. M.I.B. led the research and all authors contributed to data collation, analysis and writing the paper.

Competing Interests

The authors declare no competing interests.

Additional Information

Supplementary information is available for this paper as Supplementary Figure 1 and Supplementary Table 1.

Correspondence and requests for materials should be addressed to M.I.B.

References

1. Marciniak, S. & Perry, G. H. Harnessing ancient genomes to study the history of human adaptation. *Nat. Rev. Genet.* **18**, 659–674 (2017).
2. Crabtree, S. A., Dunne, J. A. & Wood, S. N. Ecological networks and archaeology. *Antiquity (in press)*.
3. Roopnarine, P. D. Humans are apex predators. *Proc. Natl. Acad. Sci.* **111**, E796–E796 (2014).
4. Dunne, J. A. *et al.* The roles and impacts of human hunter-gatherers in North Pacific marine food webs. *Sci. Rep.* **6**, 21179 (2016).
5. Laland, K. N. & O'Brien, M. J. Niche construction theory and archaeology. *J. Archaeol. Method Theory* **17**, 303–322 (2010).
6. Schmitt, J. *et al.* Carbon isotope constraints on the deglacial CO₂ rise from ice cores. *Science* **336**, 711–714 (2012).

7. Bonhommeau, S. *et al.* Eating up the world's food web and the human trophic level. *Proc. Natl. Acad. Sci.* **110**, 20617–20620 (2013).
8. Schoeninger, M. J. & Moore, K. Bone stable isotope studies in archaeology. *J. World Prehistory* **6**, 247–296 (1992).
9. DeNiro, M. J. Postmortem preservation and alteration of in vivo bone collagen isotope ratios in relation to palaeodietary reconstruction. *Nature* **317**, 806–809 (1985).
10. Hedges, R. E. M. & Reynard, L. M. Nitrogen isotopes and the trophic level of humans in archaeology. *J. Archaeol. Sci.* **34**, 1240–1251 (2007).
11. Salazar-García, D. C., Romero, A., García-Borja, P., Subirà, M. E. & Richards, M. P. A combined dietary approach using isotope and dental buccal-microwear analysis of human remains from the Neolithic, Roman and Medieval periods from the archaeological site of Tossal de les Basses (Alicante, Spain). *J. Archaeol. Sci. Rep.* **6**, 610–619 (2016).
12. Goude, G. & Fontugne, M. Carbon and nitrogen isotopic variability in bone collagen during the Neolithic period: Influence of environmental factors and diet. *J. Archaeol. Sci.* **70**, 117–131 (2016).
13. Barrientos, G., Catella, L. & Morales, N. S. A journey into the landscape of past feeding habits: Mapping geographic variations in the isotope ($\delta^{15}\text{N}$) -inferred trophic position of prehistoric human populations. *Quat. Int.* S1040618220300240 (2020) doi:10.1016/j.quaint.2020.01.023.
14. Guiry, E. Complexities of Stable Carbon and Nitrogen Isotope Biogeochemistry in Ancient Freshwater Ecosystems: Implications for the Study of Past Subsistence and Environmental Change. *Front. Ecol. Evol.* **7**, 313 (2019).
15. O'Connell, T. C. & Hedges, R. E. M. Investigations into the effect of diet on modern human hair isotopic values. *Am. J. Phys. Anthropol.* **108**, 409–425 (1999).
16. Lehn, C., Mützel, E. & Rossmann, A. Multi-element stable isotope analysis of H, C, N and S in hair and nails of contemporary human remains. *Int. J. Legal Med.* **125**, 695–706 (2011).
17. O'Connell, T. C., Kneale, C. J., Tasevska, N. & Kuhnle, G. G. C. The diet-body offset in human nitrogen isotopic values: A controlled dietary study. *Am. J. Phys. Anthropol.* **149**, 426–434 (2012).
18. Hülsemann, F. *et al.* Global spatial distributions of nitrogen and carbon stable isotope ratios of modern human hair: Global human carbon and nitrogen isotope ratios. *Rapid Commun. Mass Spectrom.* **29**, 2111–2121 (2015).
19. Reynard, L. M., Burt, N., Koon, H. E. C. & Tuross, N. Limits and possibilities in the geolocation of humans using multiple isotope ratios (H, O, N, C) of hair from east coast cities of the USA. *Isotopes Environ. Health Stud.* **52**, 498–512 (2016).
20. Bartelink, E. J., Berg, G. E., Beasley, M. M. & Chesson, L. A. Application of stable isotope forensics for predicting region of origin of human remains from past wars and conflicts: Human remains from past wars and conflicts. *Ann. Anthropol. Pract.* **38**, 124–136 (2014).
21. Valenzuela, L. O., Chesson, L. A., O'Grady, S. P., Cerling, T. E. & Ehleringer, J. R. Spatial distributions of carbon, nitrogen and sulfur isotope ratios in human hair across the central United States. *Rapid*

- Commun. Mass Spectrom.* **25**, 861–868 (2011).
22. Stephens, L. *et al.* Archaeological assessment reveals Earth's early transformation through land use. *Science* **365**, 897–902 (2019).
 23. Bol, R. & Pflieger, C. Stable isotope (^{13}C , ^{15}N and ^{34}S) analysis of the hair of modern humans and their domestic animals. *Rapid Commun. Mass Spectrom.* **16**, 2195–2200 (2002).
 24. Ellegård, L. *et al.* Distinguishing vegan, vegetarian, and omnivorous diets by hair isotopic analysis. *Clin. Nutr.* **38**, 2949–2951 (2019).
 25. Umezaki, M. *et al.* Association between sex inequality in animal protein intake and economic development in the Papua New Guinea highlands: The carbon and nitrogen isotopic composition of scalp hair and fingernail: Nitrogen and carbon isotopic composition in PNG. *Am. J. Phys. Anthropol.* **159**, 164–173 (2016).
 26. Casey, M. M. & Post, D. M. The problem of isotopic baseline: Reconstructing the diet and trophic position of fossil animals. *Earth-Sci. Rev.* **106**, 131–148 (2011).
 27. Handley, L. L. *et al.* The ^{15}N natural abundance ($\delta^{15}\text{N}$) of ecosystem samples reflects measures of water availability. *Funct. Plant Biol.* **26**, 185 (1999).
 28. Still, C. J., Berry, J. A., Collatz, G. J. & DeFries, R. S. Global distribution of C_3 and C_4 vegetation: Carbon cycle implications. *Glob. Biogeochem. Cycles* **17**, 6-1-6–14 (2003).
 29. Murphy, B. P. & Bowman, D. M. J. S. The carbon and nitrogen isotope composition of Australian grasses in relation to climate: *Carbon and nitrogen isotopes in grasses*. *Funct. Ecol.* **23**, 1040–1049 (2009).
 30. Kohn, M. J. Carbon isotope compositions of terrestrial C_3 plants as indicators of (paleo)ecology and (paleo)climate. *Proc. Natl. Acad. Sci.* **107**, 19691–19695 (2010).
 31. Craine, J. M. *et al.* Ecological interpretations of nitrogen isotope ratios of terrestrial plants and soils. *Plant Soil* **396**, 1–26 (2015).
 32. Cornwell, W. K. *et al.* Climate and soils together regulate photosynthetic carbon isotope discrimination within C_3 plants worldwide. *Glob. Ecol. Biogeogr.* **27**, 1056–1067 (2018).
 33. Sanseverino, A. M., Bastviken, D., Sundh, I., Pickova, J. & Enrich-Prast, A. Methane carbon supports aquatic food webs to the fish level. *PLoS ONE* **7**, e42723 (2012).
 34. 10.1007/978-90-481-3354-3_14
Graham, B. S., Koch, P. L., Newsome, S. D., McMahon, K. W. & Aurioles, D. Using isoscapes to trace the movements and foraging behavior of top predators in oceanic ecosystems. in *Isoscapes* (eds. West, J. B., Bowen, G. J., Dawson, T. E. & Tu, K. P.) 299–318 (Springer Netherlands, 2010). doi:10.1007/978-90-481-3354-3_14.
 35. Magozzi, S., Yool, A., Vander Zanden, H. B., Wunder, M. B. & Trueman, C. N. Using ocean models to predict spatial and temporal variation in marine carbon isotopes. *Ecosphere* **8**, e01763 (2017).
 36. Wainright, S. C., Haney, J. C., Kerr, C., Golovkin, A. N. & Flint, M. V. Utilization of nitrogen derived from seabird guano by terrestrial and marine plants at St. Paul, Pribilof Islands, Bering Sea, Alaska. *Mar.*

- Biol.* **131**, 63–71 (1998).
37. Zanden, M. J. V. & Rasmussen, J. B. Variation in $\delta^{15}\text{N}$ and $\delta^{13}\text{C}$ trophic fractionation: Implications for aquatic food web studies. *Limnol. Oceanogr.* **46**, 2061–2066 (2001).
 38. Layman, C. A. *et al.* Applying stable isotopes to examine food-web structure: an overview of analytical tools. *Biol. Rev.* **87**, 545–562 (2012).
 39. Szpak, P. Complexities of nitrogen isotope biogeochemistry in plant-soil systems: implications for the study of ancient agricultural and animal management practices. *Front. Plant Sci.* **5**, (2014).
 40. Lamb, A. L., Evans, J. E., Buckley, R. & Appleby, J. Multi-isotope analysis demonstrates significant lifestyle changes in King Richard III. *J. Archaeol. Sci.* **50**, 559–565 (2014).
 41. Jones, J. & Britton, K. Multi-scale, integrated approaches to understanding the nature and impact of past environmental and climatic change in the archaeological record, and the role of isotope zooarchaeology. *J. Archaeol. Sci. Rep.* **23**, 968–972 (2019).
 42. Szpak, P., Millaire, J.-F., White, C. D. & Longstaffe, F. J. Influence of seabird guano and camelid dung fertilization on the nitrogen isotopic composition of field-grown maize (*Zea mays*). *J. Archaeol. Sci.* **39**, 3721–3740 (2012).
 43. Essington, T. E., Beaudreau, A. H. & Wiedenmann, J. Fishing through marine food webs. *Proc. Natl. Acad. Sci.* **103**, 3171–3175 (2006).
 44. Tsiafouli, M. A. *et al.* Intensive agriculture reduces soil biodiversity across Europe. *Glob. Change Biol.* **21**, 973–985 (2015).
 45. Heleno, R. H., Ripple, W. J. & Traveset, A. Scientists' warning on endangered food webs. *Web Ecol.* **20**, 1–10 (2020).
 46. Bateman, A. S. & Kelly, S. D. Fertilizer nitrogen isotope signatures. *Isotopes Environ. Health Stud.* **43**, 237–247 (2007).
 47. Lu, C. & Tian, H. Global nitrogen and phosphorus fertilizer use for agriculture production in the past half century: shifted hot spots and nutrient imbalance. *Earth Syst. Sci. Data* **9**, 181–192 (2017).
 48. Schroeder, H., O'Connell, T. C., Evans, J. A., Shuler, K. A. & Hedges, R. E. M. Trans-Atlantic slavery: Isotopic evidence for forced migration to Barbados. *Am. J. Phys. Anthropol.* **139**, 547–557 (2009).
 49. Qaim, M. Globalisation of agrifood systems and sustainable nutrition. *Proc. Nutr. Soc.* **76**, 12–21 (2017).
 50. Spinoni, J., Vogt, J., Naumann, G., Carrao, H. & Barbosa, P. Towards identifying areas at climatological risk of desertification using the Köppen-Geiger classification and FAO aridity index: Towards identifying areas at climatological risk of desertification. *Int. J. Climatol.* **35**, 2210–2222 (2015).
 51. Bol, R. *et al.* The natural abundance of ^{13}C , ^{15}N , ^{34}S and ^{14}C in archived (1923–2000) plant and soil samples from the Askov long-term experiments on animal manure and mineral fertilizer. *Rapid Commun. Mass Spectrom.* **19**, 3216–3226 (2005).

52. Bogaard, A., Heaton, T. H. E., Poulton, P. & Merbach, I. The impact of manuring on nitrogen isotope ratios in cereals: archaeological implications for reconstruction of diet and crop management practices. *J. Archaeol. Sci.* **34**, 335–343 (2007).
53. Stevens, R. E., Lister, A. M. & Hedges, R. E. M. Predicting diet, trophic level and palaeoecology from bone stable isotope analysis: a comparative study of five red deer populations. *Oecologia* **149**, 12–21 (2006).
54. Doppler, T. *et al.* Landscape opening and herding strategies: Carbon isotope analyses of herbivore bone collagen from the Neolithic and Bronze Age lakeshore site of Zurich-Mozartstrasse, Switzerland. *Quat. Int.* **436**, 18–28 (2017).
55. Crabtree, S. A., Bird, D. W. & Bird, R. B. Subsistence transitions and the simplification of ecological networks in the western desert of Australia. *Hum. Ecol.* **47**, 165–177 (2019).
56. Williams, R. J. & Martinez, N. D. Limits to trophic levels and omnivory in complex food webs: Theory and data. *Am. Nat.* **163**, 458–468 (2004).
57. Cerling, T. E. *et al.* Global vegetation change through the Miocene/Pliocene boundary. *Nature* **389**, 153–158 (1997).
58. Crabtree, S. A., Vaughn, L. J. S. & Crabtree, N. T. Reconstructing ancestral pueblo food webs in the southwestern United States. *J. Archaeol. Sci.* **81**, 116–127 (2017).
59. Pauli, J. N. *et al.* Opinion: Why we need a centralized repository for isotopic data. *Proc. Natl. Acad. Sci.* **114**, 2997–3001 (2017).
60. Bartley, T. J. *et al.* Food web rewiring in a changing world. *Nat. Ecol. Evol.* **3**, 345–354 (2019).
61. Romanuk, T. N., Zhou, Y., Valdovinos, F. S. & Martinez, N. D. Robustness trade-offs in model food webs. in *Advances in Ecological Research* vol. 56 263–291 (Elsevier, 2017).
62. Reynard, L. M. & Tuross, N. The known, the unknown and the unknowable: weaning times from archaeological bones using nitrogen isotope ratios. *J. Archaeol. Sci.* **53**, 618–625 (2015).
63. Graven, H. *et al.* Compiled records of carbon isotopes in atmospheric CO₂ for historical simulations in CMIP6. *Geosci. Model Dev.* **10**, 4405–4417 (2017).
64. Rousseeuw, P. J., Ruts, I. & Tukey, J. W. The bagplot: A bivariate boxplot. *Am. Stat.* **53**, 382–387 (1999).
65. Bocherens, H. & Drucker, D. Trophic level isotopic enrichment of carbon and nitrogen in bone collagen: case studies from recent and ancient terrestrial ecosystems. *Int. J. Osteoarchaeol.* **13**, 46–53 (2003).

Figures

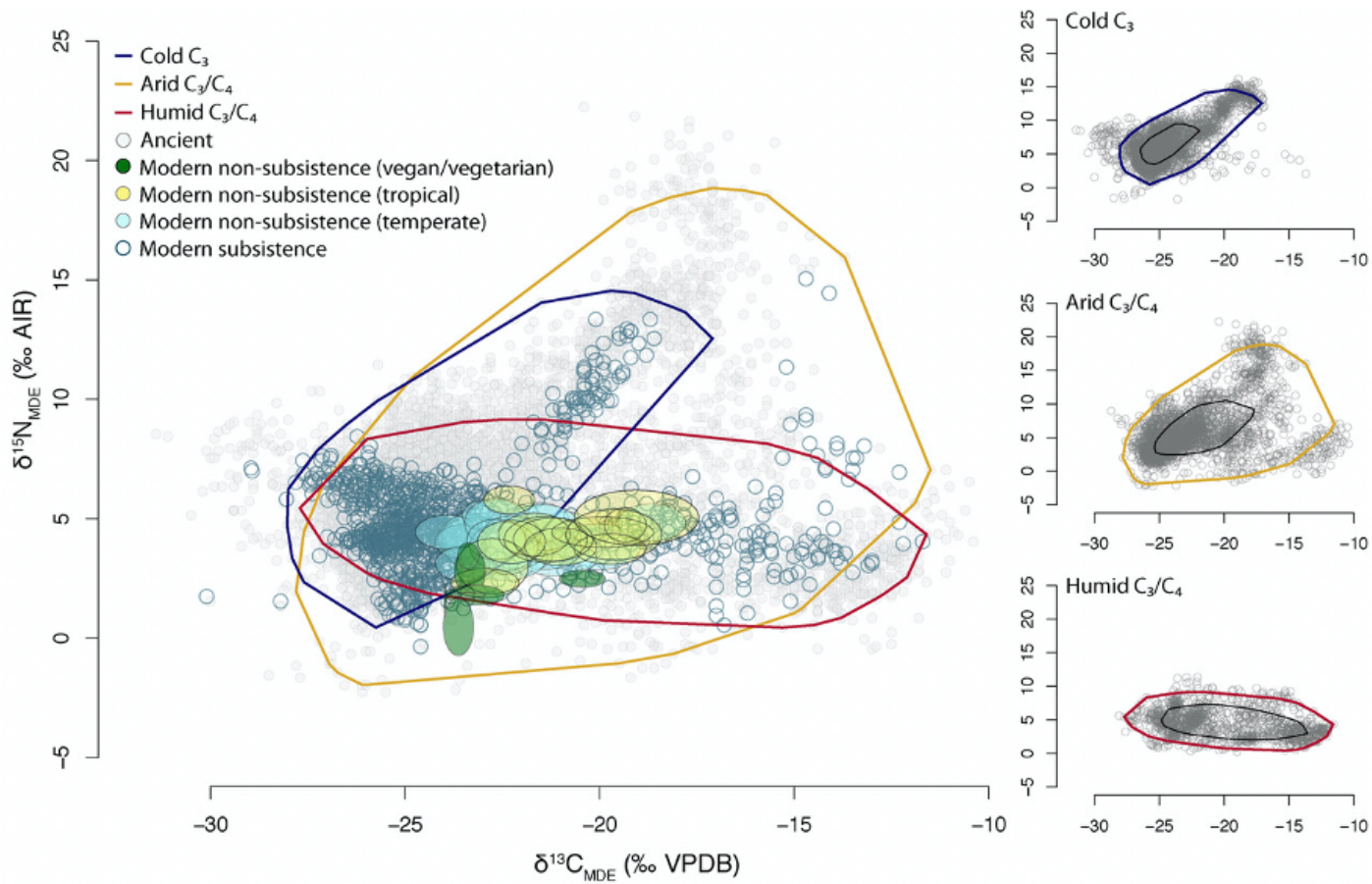


Figure 1

Bagplots of $\delta^{13}\text{C}_{\text{MDE}}$ and $\delta^{15}\text{N}_{\text{MDE}}$ pairs for ancient individuals (grey) within cold C₃ (dark blue), arid C₃/C₄ (orange) and humid C₃/C₄ (red) environs. Black contours in the small side panels enclose 50% of individuals, coloured contours on all panels enclose 95% of individuals. $\delta^{13}\text{C}_{\text{MDE}}$ and $\delta^{15}\text{N}_{\text{MDE}}$ of modern subsistence individuals (dark blue), tropical (yellow) and temperate (light blue) non-subsistence populations are shown overlain on the ancient data. Modern non-subsistence individuals are plotted as ellipses representing the population μ (ellipse centre) and 2σ (ellipse extent). Vegans/vegetarians within this last category are highlighted by green shaded ellipses. The modern non-subsistence data is plotted on an expanded scale by region in Supplementary Figure 1.

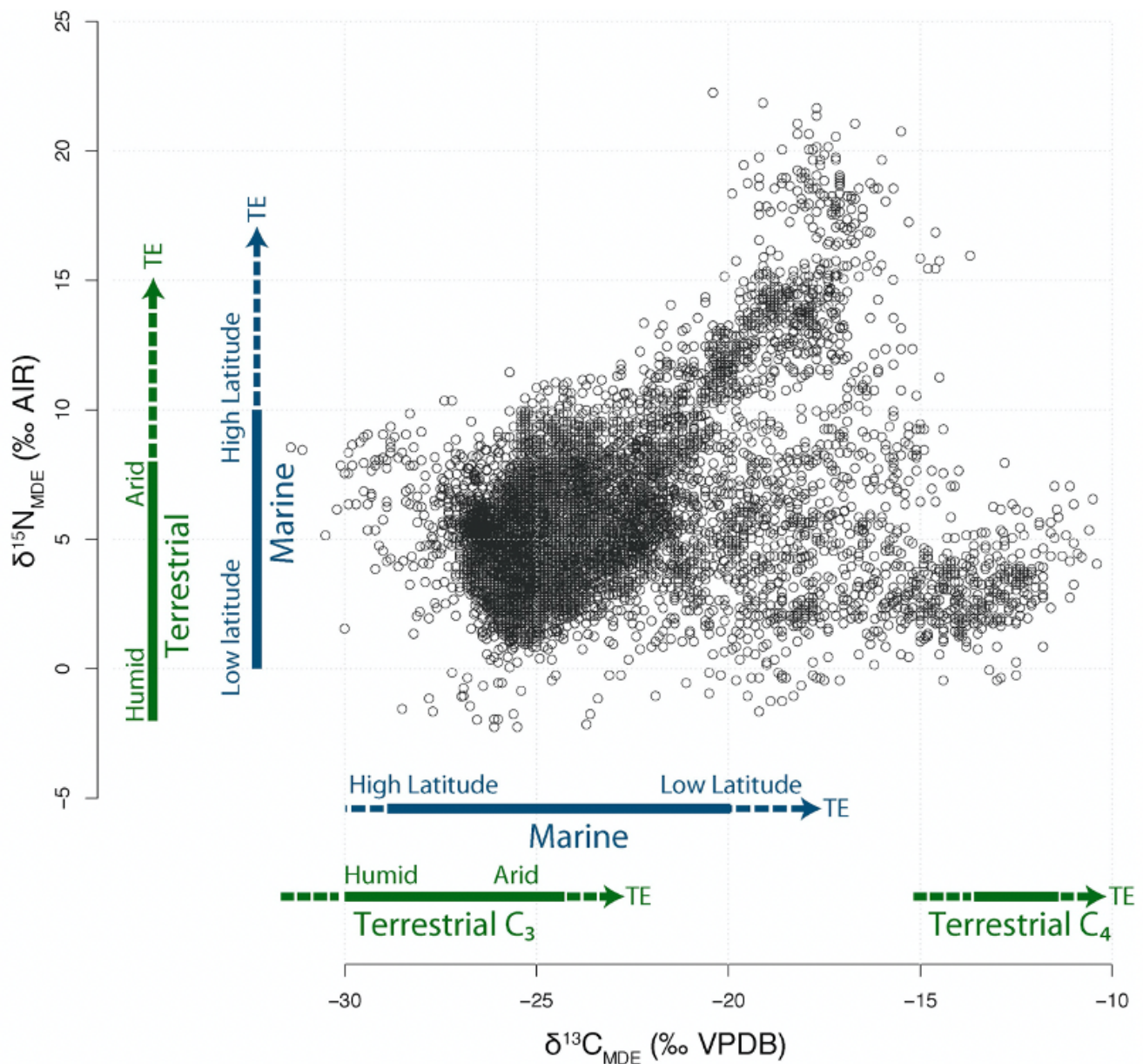


Figure 2

Modern Diet Equivalent (MDE) data for all ancient individuals (grey points) representing the full dietary spectrum. Terrestrial (green) and Marine (blue) plant/animal $\delta^{13}\text{C}_{\text{MDE}}$ and $\delta^{15}\text{N}_{\text{MDE}}$ ranges are given (solid lines) for comparison. Dashed arrows indicate where Tropic Enrichment (TE) extends this range to higher values. The marine range for primary production taken from Graham et al.³⁴ for nitrogen and Magozzi et al.³⁵ for carbon. The terrestrial range of values for primary production for shown for carbon^{29,30,32,57} and for nitrogen^{27,29,31}.

Supplementary Files

This is a list of supplementary files associated with this preprint. Click to download.

- [SupplementaryFigure1.docx](#)
- [SupplementaryTable1.xlsx](#)